

URBAN ATLAS – DLR PROCESSING CHAIN FOR ORTHORECTIFICATION OF PRISM AND AVNIR-2 IMAGES AND TERRASAR-X AS POSSIBLE GCP SOURCE

Mathias Schneider¹, Rupert Müller¹, Thomas Krauss¹, Peter Reinartz¹, Bianca Hörsch², Siegfried Schmuck²

¹German Aerospace Center (DLR), Remote Sensing Technology Institute, D-82234 Wessling, Germany

e-mail: {Mathias.Schneider, Rupert.Mueller, Thomas.Krauss, Peter.Reinartz}@dlr.de

²ESA-ESRIN European Space Agency, Via Galileo Galilei, Casella Postale 64, 00044 Frascati (Rome), Italy

e-mail: {Bianca.Hoersch, Siegfried.Schmuck}@esa.int

ABSTRACT:

In the first part of this paper, the semi-automatic processing chain established at the DLR for the processing of PRISM and AVNIR-2 data in the framework of Urban Atlas is described. Although the processing chain was designed to be fully automatic, the lack of a sufficient accurate reference image necessitates the manual measurement of ground control points (GCP) from digital maps and aerial imagery to fulfill the accuracy requirements of 5 m RMSE in case of PRISM images. In case of AVNIR-2 images, the internal reference database available at DLR was sufficient accurate to allow for an automatic GCP generation. Since no ground truth was available, the included quality check uses different criteria to allow for a quality measure for each image.

In the second part of the paper, the accuracy of the orthorectified scenes is analyzed. Up to now, more than 200 PRISM and 100 AVNIR-2 scenes for 43 European cities are processed. The overall accuracy statistics are presented and additionally some single scenes are evaluated in areas where additional ground truth is available.

In further investigations, TerraSAR-X data was evaluated regarding its potential as source for GCPs. The very high geometric accuracy of geocoded data of the TerraSAR-X satellite has been shown in several investigations and thus qualifies the data as GCP source. Different methods of retrieving GCPs from TerraSAR-X data have been evaluated in the third part of the paper: manual measurements or local image matching using mutual information. By adjustment calculations, falsely matched points can be eliminated and an optimal improvement can be found. After the orthorectification of the PRISM data using these improvements, the results are compared to PRISM data that were orthorectified using conventional ground control information from GPS measurements.

1 INTRODUCTION

In order to encourage more sustainable development in urban conglomerations and to evaluate the compliance and success of planning measures, detailed knowledge of urban land use is essential for monitoring and analyzing changes on a geolocated basis. The GMES Land Information Service Urban Atlas is providing this knowledge. Various EO data such as SPOT4/5, Formosat-2, Quickbird, as well as ALOS PRISM and AVNIR-2 data serve as input data, to compile a total of 318 major European cities. The preprocessing of the ALOS data is done by the Remote Sensing Technology Institute at the DLR (German Aerospace Center). In this paper, the DLR processing chain is described, including manual GCP measurement and quality control. The accuracy of the orthorectified scenes is presented in overall statistics and for some single scenes.

During the project, the difficulty of providing GCPs for high-resolution satellite imagery became obvious. In this project, digital maps, aerial images and previously orthorectified satellite imagery with a high precision are used. However, additional GCP sources are necessary in the future. The very high geometric accuracy of geocoded data of the TerraSAR-X satellite has been shown in several investigations (e.g. Nonaka et al., 2008). It is due to the fact that it measures distances, which are mainly dependent on the position of the satellite and the terrain height. If the used DEM is of high accuracy, the resulting geocoded data are very precise. Therefore, the possibility of retrieving GCPs from TerraSAR-X data is examined and presented in this paper.

2 PROCESSING CHAIN

The automatic image processing chain CATENA was developed at the Remote

Sensing Technology Institute at the DLR. It is based on the in-house developed image processing software XDIBIAS and can be operated by a web-interface. It is a further development of the processing chain used for the Image2006 project (Müller et al., 2007). The data of several different satellites, such as SPOT 4/5, IRS-P6, IKONOS, QUICKBIRD, Cartosat, Geo-Eye, Rapid Eye, Worldview and ALOS can be processed. Further satellites will be included in the future. CATENA was designed to process satellite imagery fully automatically from a processing level corresponding to L1B1 for ALOS to an orthorectified scene.

2.1 Workflow in the automatic processing chain

After the import of the image and metadata, a reference scene and a DEM are extracted from respective databases. The DEM database consists of the SRTM DEM and – above 60° N and below 60° S – the ASTER Global DEM. The reference image database consists of the Image2006 dataset.

An automatic intensity based matching (Lechner, Gill, 1992) is done between satellite scene and reference image and the resulting matching points are splitted into ground control points (GCP) and independent check points (ICP) using the quality figure and the distribution over the image as criteria. The GCPs are used to improve the orientation or the RPCs respectively, depending on the satellite. In the last step, the image is orthorectified using the improved sensor model and the DEM and resampled to any given projection. For ALOS data, the algorithms are described in (Schneider et al., 2008) and (Schwind et al., 2009).

2.2 Modifications for Urban Atlas

For Urban Atlas, several modifications to the automatic processing chain became necessary, changing it into a semi-automatic processing chain.

The geometric accuracy of the reference database is in the order of 10-15 m, which is sufficient for the processing of AVNIR-2 data. However, it does not fulfill the requirement for PRISM data of 5 m absolute accuracy. Therefore, in case of PRISM data, no automatic matching is done. GCPs are measured manually from digital vector maps or aerial images. After the insertion of these GCPs into CATENA, the processing continues and orthoimages are computed both in

Lambert Azimuthal Equal Area (LAEA) and UTM projection.

After the orthorectification, the quality of the orthorectified scene can be assessed in a manual quality check.

2.3 Quality check

At the end of the processing chain, a manual quality check is carried out for each orthorectified scene. This is done via a questionnaire, in which different criteria are checked. Since in most cases no independent dataset is available against which the orthoimages can be checked, several criteria are used that are each alone not significant enough. The questionnaire includes six sections:

Reference image database:

A reference image is always extracted from the database, no matter if it is used for a matching or not. In this section, the reference image is checked regarding cloud coverage, seamlines etc. which might obstruct a matching.

DEM:

In this section, the extracted DEM is checked if it covers the complete image area and if it contains seamlines or holes.

Orthorectified scene:

In this section, the cloud coverage is given in 1/8 steps. The radiometry is checked and the possible error resulting from off-nadir view and DEM accuracy is calculated. The orthorectified scene is checked against the reference image via an overlay of the scenes. However, as the geolocation accuracy of the reference image is in the order of 10 – 15 m, in case of PRISM images shifts of several pixels are possible.

Matching/GCPs/ICPs:

In this section, the GCP distribution and the RMSE values at the GCPs are checked. In case of AVNIR-2 images, also the RMSE values at the ICPs and a residual plot are included in the quality check.

Neighboring images:

In this section, the consistency of the orthorectified scene to its neighbors is checked via an overlay.

OpenStreetMap overlay:

In this section, vector data is downloaded from the OpenStreetMap project and is superimposed on the orthorectified scene. However, the accuracy and the source of the vector data are unknown and the amount of available vector data differs from city to city. Figure 1 shows an example of OpenStreetMap vector data superimposed on a PRISM scene of Marseille. In this example, there is enough vector data available and it fits well on the orthorectified scene.

Each of the described sections can be marked as OK, problematic or not applicable and the overall quality is given as the quotient of OKs and total number of sections applicable in percent.

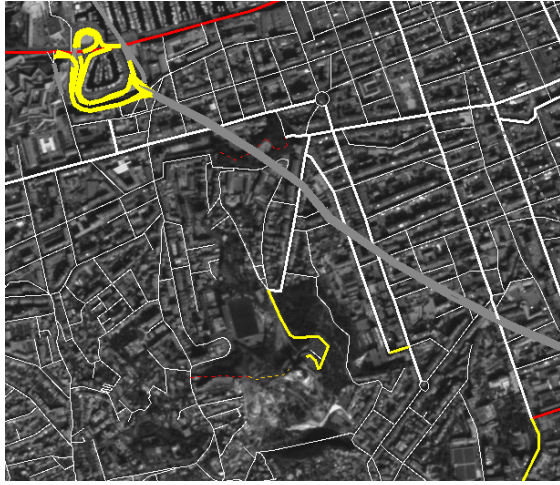


Figure 1: Overlay of OpenStreetMap vector data on a PRISM scene of Marseille

3 Accuracy and statistics

In the first two slices, scenes over 43 European cities were processed including 83 AVNIR-2 scenes and 196 PRISM scenes. Currently, the third slice is processed, consisting of up to now 144 PRISM scenes and 85 AVNIR-2 scenes over 25 European cities. In the following chapters, only scenes from the first two slices are analyzed.

3.1 Accuracy analysis for AVNIR-2 scenes

As described in chapter 2.1, in case of AVNIR-2 imagery, the GCPs are extracted by an automatic matching producing also ICPs. Figure 2 shows the RMSE values at these ICPs in X, Y and the combined value. The number of extracted ICPs varies for each image between 26 and 27515 with a mean number of approximately 5000 ICPs per image.

The RMSE values in X-direction are all between 3.5 m and 12.1 m. In Y-direction, all values are between 3.9 m and 10.7 m. That means that the accuracy of the orthorectified AVNIR-2 scenes with respect to the used reference is in the order of about one pixel or better. In all scenes, the overlay to the neighboring images as well as the OpenStreetMap overlay returned good results. In addition, the analysis of the residual plots shows with few exceptions good results.

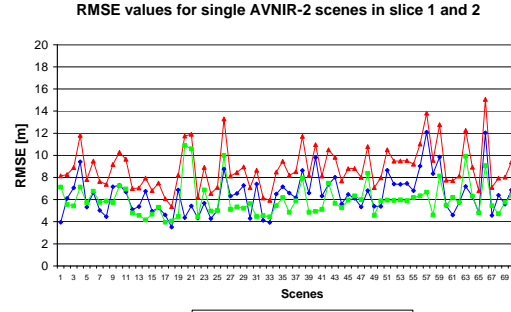


Figure 2: RMSE values at ICPs in AVNIR-2 scenes.

However, these exceptions are due to a bad mosaicking of the reference scenes at these locations and do not indicate a bad quality. In summary, the analysis of the AVNIR-2 images with respect to both the reference images and to other data sources like OpenStreetMap returns a remarkably good accuracy.

3.2 Accuracy analysis for PRISM scenes

In contrast to the AVNIR-2 scenes, in case of PRISM imagery no ICPs exist as a quality measure. Therefore, for an overall analysis, the RMSE values at the GCPs were analyzed (Figure 3).

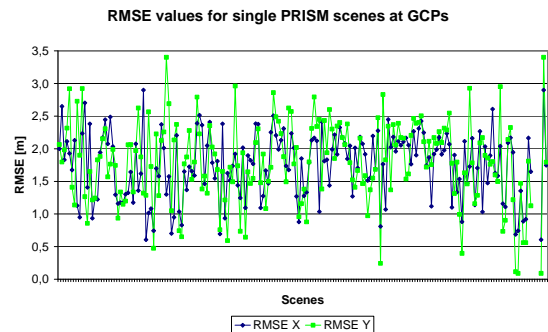


Figure 3: RMSE values at GCPs in PRISM scenes

Naturally, the RMSE values are very small at the GCPs, between 0.1 and 3.4 m and with an average of 1.75 m.

For five scenes in Germany, aerial images became available after the processing. These images were used for an independent accuracy assessment. Therefore, the orthorectified scenes were matched to the aerial images and the coordinates of the matched points in both images were compared. Table 1 shows the results of the analysis.

	X	Y
Scene	ALPSMN129732570	
Mean	-1.57	-0.35
Standard dev. [m]	2.06	2.08
RMSE [m]	2.59	2.11
No. of points	25693	

	X	Y
Scene	ALPSMN129732580	
Mean	-2.10	-1.51
Standard dev. [m]	2.19	2.19
RMSE [m]	3.03	2.66
No. of points	10080	

	X	Y
Scene	ALPSMN067592575	
Mean	-0.29	-2.36
Standard dev. [m]	2.50	2.45
RMSE [m]	2.52	3.40
No. of points	9645	

	X	Y
Scene	ALPSMN067592570	
Mean	-0.30	-4.21
Standard dev. [m]	2.24	1.70
RMSE [m]	2.26	4.54
No. of points	20910	

	X	Y
Scene	ALPSMN078532580	
Mean	-0.17	-2.47
Standard dev. [m]	2.45	2.61
RMSE [m]	2.45	3.59
No. of points	9370	

Table 1: Accuracy analysis for five PRISM scenes in Germany after a matching of orthorectified scenes and aerial images

Additionally, for a scene over Marseille, France 25 GPS measured points were available. Eight of these points were used as GCPs in the processing. Table 2 shows the statistics at the 25 GPS points measured manually in the orthorectified scene.

	X	Y
Scene	ALPSMN060152725	
Mean	-0.73	3.40
Standard dev. [m]	3.04	3.33
RMSE [m]	3.07	4.72
No. of points	25	

Table 2: Accuracy analysis for 25 GPS points in a PRISM scene

The RMSE values in all images are in the order of one, maximum two pixels both in x- and y-direction. Thus, the required accuracy is reached.

Analyzing both the RMSE values at the GCPs and the matching between orthorectified scenes and aerial images, it can be noticed that the RMSE values in y-direction are in most scenes larger than the ones in x-direction. This is due to the better accuracy of ALOS exterior orientation auxiliary data in x-direction.

4 TerraSAR-X imagery as possible source for GCPs

During the Urban Atlas project, it became obvious, that a global or at least large-area reference for high-resolution satellite imagery would be very valuable. While this reference exists for imagery with a resolution of 10 - 30 m with the USGS Landsat-database and e.g. the Image 2000 and Image 2006 projects in Europe, it is still missing for higher resolutions. As the very high geometric accuracy of geocoded data of the TerraSAR-X satellite has been shown in several investigations, it could serve as a source for GCP extraction and thus improve the orthorectification of optical satellite data.

In order to extract GCPs, homologous points in the two images have to be found. This can be done either by manual/visual measurements, or by automatic techniques using multimodal image matching. Since the image information of both data sets is very different, this is not always a straightforward procedure. Both techniques are shortly described and examples as well as results are given.

4.1 Manual measurements

When looking at a TerraSAR-X scene, the human eye can interpret many objects/features almost as well as in optical images. Thus, one of our first thoughts was to try a manual measurement of conjugate points and use them as GCPs. However, the different characteristics of optical and radar imagery have to be considered. Especially the typical radar effects like foreshortening, shadowing etc. should be accounted for when selecting GCPs manually. Selected GCPs should be situated in flat terrain and they should not be surrounded by trees or high buildings. During the tests, street crossings in agricultural areas as well as the center of roundabouts turned out to be good GCPs. However, the measurement is still very challenging and needs an experienced operator.

In a test, the potential of manual GCP measurement was examined. Therefore, a test area near Marseille, France, was chosen. An ALOS PRISM nadir scene recorded on March

12, 2007 with a 2.5 meter resolution and a TerraSAR-X Stripmap scene recorded on April 20, 2009 with a resolution of 1.25 meter were used for the test. Additionally, 25 GCPs measured with GPS were available.

For the test, 10 conjugate points were measured in both the TerraSAR-X and the PRISM scene. These points were used as GCPs to correct the orientation of the PRISM scene as described in section 4. The PRISM scene was then orthorectified using the corrected orientation. Another orthoimage was generated by correcting the orientation using eight of the GPS points as GCPs. Figure 4 shows an overlay of these orthoimages.



Figure 4: Overlay of orthoimages. The blue and green channels show the orthoimage created with the GPS points, the red channel the one created using the TerraSAR-X points as GCPs. There are only very small visually detectable color edges found.

The grey color indicates a very high consistency of both orthorectified images. This holds also true in mountainous areas. In order to assess the geometric accuracy of the orthorectified scene using GCP information extracted from the TerraSAR-X imagery, the GPS points were manually measured in the orthoimage. Table 3 shows the results.

	x	y
Mean [m]	-1.7	-3.4
Standard deviation [m]	2.6	3.0
RMSE [m]	3.1	4.5

Table 3: Statistics on 25 check points (GPS measurements)

4.2 SAR/optical image matching

Mutual information has evolved from the field of information theory and describes a statistical dependence between two random variables expressed in terms of variable entropies. In case Shannon entropy (additive in nature) is

selected to represent the individual variable information, mutual information between two variables A and B is defined as in (Wachowiak et al., 2002):

$$MI(A, B) = H(A) + H(B) - H(A, B)$$

Where $H(A)$ and $H(B)$ are the Shannon entropies of A and B respectively and $H(A, B)$ is the joint entropy of A and B. Matching points are found by maximization of $MI(A, B)$ in the equation above. The applicability of mutual information as registration metric for high-resolution satellite imagery (esp. from radar and optical sources) in urban areas was highlighted e.g. in (Suri, Reinartz, 2009). In this test, the refined algorithms described in (Suri, Reinartz, 2009) were used to fine match TerraSAR-X and ALOS image and thus to extract GCPs for improving the ALOS sensor model.

To evaluate the performance of the MI based approach, the same dataset as for the manual GCP measurements was used.

In a first step, an equidistant grid of points in the original PRISM image is generated. To facilitate MI matching of these points with the reference TerraSAR-X scene, the PRISM image is orthorectified using the uncorrected attitude information (Mean shift compared to the reference GPS points: -24.7 m in x; -84.44 m in y). After the MI matching, the found matches are used to estimate more accurate attitude angles. Additionally, during this step wrong and inaccurate matches are eliminated. Finally, the improved sensor model is used to orthorectify the PRISM scene.

	x	y
Mean [m]	-2.8	-8.0
Standard deviation [m]	2.6	2.0
RMSE [m]	3.8	8.2

Table 4: Statistics on 25 check points (GPS measurements)

For the MI statistic computation a window with a size of 400x400 pixels is employed, using a Sextic B-Spline Kernel for joint histogram estimation (Suri, Reinartz, 2008). 122 grid points were generated automatically, out of which 109 remained after MI matching (selected on the basis of individual match consistency). The corrections obtained by MI are shown in Figure 5. During the sensor model improvement step another 38 points were discarded, finally leading to 71 remaining matches with a RMSE of these points 0.73 pixel in x and 0.86 pixel in y relative to the computed model.

When compared to the 25 independent high precision GPS points a mean deviation of -2.8 m and -8.0 m in x and y respectively was obtained (Table 4). While the mean deviation

has not yet achieved results as good as those obtained manually, the comparably low standard deviation (x : 2.6 m; y : 2.0 m) indicates a good matching consistency.

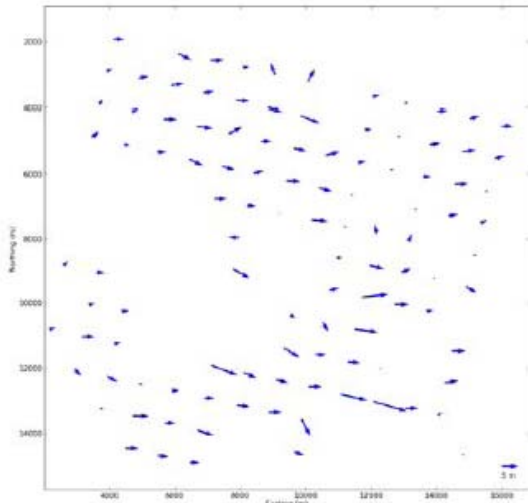


Figure 5: Shifts of matches computed by MI compared to their initial position (arrow lengths are scaled by a factor 100)

5 Conclusion

In this paper, the fully automatic processing chain for the orthorectification of ALOS PRISM and AVNIR-2 imagery in the frame of the Urban Atlas project established at the DLR is presented. The modifications to the processing chain for this specific project converting it to be semi-automatic are presented and the manual quality assessment is highlighted.

The accuracy of the orthorectified scenes is assessed and analyzed both for AVNIR-2 and PRISM data. In the examined scenes, an accuracy in the order of approximately one pixel for both sensors is found. This shows that ALOS imagery is fully suitable for high resolution mapping applications. However, the need for a high resolution reference became apparent. The manual measurement of the GCPs is a tedious and time consuming work and it is partly very difficult to obtain the GCP sources like digital maps and aerial imagery etc. depending on the region of interest.

Therefore, in the third part of the paper, a possible additional GCP source is examined. Due to the very high geometric accuracy and the large coverage of TerraSAR-X data, it could serve as a GCP source. It is shown that with manual GCP measurement, an accuracy comparable to GPS measurements can be reached. Using automatic image matching techniques based on mutual information, the accuracy is slightly lower than in case of manual measurements. However, the methods

will be further refined in ongoing studies and it is likely that in the near future TerraSAR-X data can serve as a source for a worldwide high precision geolocation of HR and VHR satellite images.

6 References

- T. Nonaka , Y. Ishizuka , N. Yamane , T. Shibayama , S. Takagishi , T. Sasagawa, (2008): *Evaluation of the Geometric Accuracy of TerraSAR-X*, XXI ISPRS Congress Beijing, China, 2008-07-03 - 2008-07-11, 6p.
- R. Müller, T. Krauß, M. Lehner, P. Reinartz, (2007): *Automatic Production Of A European Orthoimage Coverage Within The GMES Land Fast Track Service Using Spot 4/5 And Irs-P6 Liss III Data*, ISPRS Conference Proceedings, Volume XXXVI, ISPRS Workshop Hannover, Germany, May 2007, 6 p.
- M. Lehner, R. S. Gill (1992): *Semi-automatic derivation of digital elevation models from stereoscopic 3-line scanner data*, IAPRS Vol. 29 part B4, Washington, USA, pp 68-75, 1992
- Schneider, M. und Lehner, M. und Müller, R. und Reinartz, P. (2009): *Stereo Evaluation of ALOS/PRISM Data on ESA-AO Test Sites - First DLR Results*, ALOS PI Symposium 2008, 2008-11-03 - 2008-11-07, Rhodes (Greece).
- P. Schwind, M. Schneider, G. Palubinskas, T. Storch, R. Müller, and R. Richter (2009): *Processors for ALOS Optical Data: Deconvolution, DEM Generation, Orthorectification, and Atmospheric Correction*, IEEE Transactions on Geoscience and Remote Sensing, IEEE, USA, in press.
- M.P. Wachowiak, R. Smolikova, G.D. Tourassi, A.S. Elmaghraby, 2002: *Generalized Mutual Information as a Similarity Metric for Multimodal Biomedical Image registration*, Proc. of the EMBS/BMES 2002 Conference, Houston, TX, 1005-1006
- S. Suri, P. Reinartz, 2009: *On the Possibility of Intensity Based Registration for Metric Resolution SAR and Optical Imagery*, 12th AGILE International Conference on Geographic Information Science 2009 Leibniz Universität Hannover, Germany
- S. Suri, P. Reinartz, 2008: *Application of Generalized Partial Volume Estimation for Mutual Information based Registration of High Resolution SAR and Optical Imagery*, Proceedings of Fusion 2008, Cologne, Germany, June 2008, 8 p.